Bulk and surface phonon–polaritons in ternary mixed crystals

2006 J. Phys.: Condens. Matter 18 8229

(http://iopscience.iop.org/0953-8984/18/35/010)

INSTITUTE OF PHYSICS PUBLISHING JOURNAL OF PHYSICS: CONDENSED MATTER

J. Phys.: Condens. Matter **18** (2006) 8229–8239 doi:10.1088/0953-8984/18/35/010

Bulk and surface phonon–polaritons in ternary mixed crystals

J Bao[1] **and X X Liang**[1,2,3]

[1] Department of Physics, Inner Mongolia University, Hohhot 010021, People's Republic of China
[2] CCAST (World Laboratory), PO Box 8730, Beijing 100080, People's Republic of China

E-mail: xxliang@imu.edu.cn

Received 18 April 2006, in final form 12 June 2006
Published 15 August 2006
Online at stacks.iop.org/JPhysCM/18/8229

Abstract

The bulk and surface phonon–polaritons in ternary mixed crystals are investigated in the random-element-isodisplacement model and Born–Huang approximation. The numerical results of the polariton frequencies and oscillator strengths as functions of the wavevector and the composition for ternary mixed crystals $Al_xGa_{1-x}As$, $Zn_xCd_{1-x}S$, and $Ga_xIn_{1-x}N$ are obtained and discussed. It is shown that there are three propagated bands separated by two forbidden bands for the phonon–polaritons in bulk materials and two branches of surface phonon–polaritons in semi-infinite systems. The 'two-mode' and 'one-mode' behaviours of phonon–polaritons are also shown in the dispersion curves of bulk and surface phonon–polaritons.

1. Introduction

Polaritons, as a kind of hybrid modes of elementary excitations in condensed matters, have been attracting a great deal of interest since the pioneering work of Huang *et al* [1–4]. Properties of phonon–polaritons associated with lattice vibrations coupled to electromagnetic waves have been successfully studied experimentally and theoretically [5–8]. The spontaneous Raman scattering of phonon–polaritons was proposed theoretically and first analysed experimentally through the observation of the lower dispersion curve in the GaP cubic crystal by Henry and Hopfield [2]. Later, the surface phonon–polaritons in the GaAs film, as well as GaP thin slab and other materials were also observed [9–11]. Moreover, the generation, dispersion and decay of phonon–polaritons have been extensively investigated experimentally by various optical methods [12–16]. Very recently, the promising technique of terahertz (THz) time-domain spectroscopy has been used to observe phonon–polariton dispersion relations [17]. Surface phonon–polaritons have also been observed by the method of attenuated total reflection (ATR) [18, 19].

[3] Address for correspondance: Department of Physics, Inner Mongolia University, Hohhot 010021, People's Republic of China.

In recent years, the properties of ternary mixed crystals (TMCs) have attracted much attention of both theoretical and experimental scientists [20–24] because of their applications to multilayer materials of semiconductors. As was well known, the optical phonon modes in TMCs show properties quite different from those in binary crystals: there are two pairs of branches of longitudinal–transverse optical (LO–TO) phonon modes propagated in polar TMC materials [20, 25]. According to the oscillator strengths and the features of the modes, polar TMCs can be classed into 'one-mode' and 'two-mode' behaviour types. In a 'one-mode' behaviour TMC, a pair of LO–TO branches is much stronger than another in the oscillator strengths and should be the only one considered in practice. Otherwise, the two pairs of LO–TO phonon branches are both important and observable in 'two-mode' behaviour TMC systems. Naturally, the novel properties of optical vibrations in TMCs, such as the 'two-mode' behaviour and the concentration dependence of frequencies and oscillator strengths, contribute new characteristics of phonon–polaritons.

The phonon–polariton results in the infrared absorption and dielectric abnormality, etc, and concerns the developments and applications of new photoelectron devices [14–19, 26–28]. Employing polar TMCs in artificial materials can enable one to modify the vibrational and optical properties as well as the polariton characteristics of the systems in a controlled manner, and may extend their applications to devices [20–24]. However, although the polaritons of polar binary crystals are widely investigated, to the best of our knowledge, the theoretical and experimental studies of the polaritons in polar TMCs, in special surface polaritons, have been rarely reported. Further investigations on the properties of polaritons in TMC systems are therefore invoked.

One of the authors and his collaborators have theoretically investigated the optical vibrations of polar TMCs in the modified random-element-isodisplacement (MREI) approximation [25] and obtained the normal modes of optical phonons and the electron–phonon interaction Hamiltonian [29]. In the present paper we extend the previous work and discuss the bulk and surface phonon–polaritons in TMCs. The MREI approximation [25] and the Born–Huang method [1] for the optical vibrations of lattices are used in the formulation. The frequencies and the oscillator strengths of the polaritons are calculated numerically for several typical TMCs. The dispersion characteristics and their concentration dependences of the bulk and surface phonon–polaritons are discussed in detail.

2. Bulk phonon–polaritons in ternary mixed crystals

Now we first explore the properties of bulk phonon–polaritons in polar TMCs. Consider an electromagnetic wave propagated in a polar TMC $A_xB_{1-x}C$ of cubic symmetry, which couples with transverse optical (TO) modes of lattice vibrations and forms phonon–polaritons. Since the frequency of the electromagnetic wave coupling with optical phonons must be the order of magnitude of the TO phonon frequency ω_{TO}, which is related to the photons with long wavelengths compared to the lattice constant, the long-wavelength approximation will be adopted in our calculations [4]. Moreover, the dielectric function $\varepsilon(k, \omega)$ is considered as isotropic for the TMC material of cubic symmetry. The propagation of phonon–polaritons coupled with the electromagnetic radiation with the TO phonon field in the TMC can be described by linking the Maxwell's equations with the Born–Huang-like equations describing the lattice vibrations as follows:

$$\nabla \times \vec{E} = -\mu_0 \frac{\partial \vec{H}}{\partial t}, \tag{1}$$

$$\nabla \times \vec{H} = \frac{\partial}{\partial t}\left(\varepsilon_0 \vec{E} + \vec{P}\right), \tag{2}$$

$$\nabla\cdot\vec{D} = 0, \tag{3}$$

$$\nabla\cdot\vec{H} = 0, \tag{4}$$

$$\ddot{\vec{W}}_1 = b_{11}\vec{W}_1 + b_{12}\vec{W}_2 + b_{13}\vec{E}, \tag{5}$$

$$\ddot{\vec{W}}_2 = b_{21}\vec{W}_1 + b_{22}\vec{W}_2 + b_{23}\vec{E}, \tag{6}$$

$$\vec{P} = b_{31}\vec{W}_1 + b_{32}\vec{W}_2 + b_{33}\vec{E}. \tag{7}$$

Here, $\vec{W}_1 = \mu_1^{1/2}\vec{s}_1$ and $\vec{W}_2 = \mu_2^{1/2}\vec{s}_2$, where $\vec{s}_1 = (\vec{u}_A - \vec{u}_C)$ and $\vec{s}_2 = (\vec{u}_B - \vec{u}_C)$ are the relative displacements of the A–C ion and B–C ion pairs, respectively, μ_1 and μ_2 are the corresponding reduced masses. u_A, u_B, and u_C are respectively the displacements of the ions A, B, and C. $\vec{E}$, $\vec{H}$ are respectively the macroscopic electric and magnetic field and $\vec{P}$ the polarization. μ_0 and ε_0 are the vacuum magnetic permeability and the dielectric constant respectively. The dynamical coefficients b_{ij} $(i, j = 1, 2, 3)$ in equations (5)–(7) have been determined by using the macroscopic parameters of the end-member binary crystals AC ($x = 1$) and BC ($x = 0$), according to the Born–Huang procedure in the previous works [29, 30], and here we give them in the appendix.

Let us assume the solutions of equations (1)–(7) as the following form

$$\vec{W}, \vec{p}, \vec{E}, \vec{H} \propto \exp[\mathrm{i}(\vec{k}\cdot\vec{r} - \omega t)], \tag{8}$$

where ω and $\vec{k}$ are respectively the frequency and wavevector of the phonon–polaritons. Inserting the solutions of form (8) into equations (1)–(7), one can obtain the following relation between the macroscopic electric field $\vec{E}$ and the polarization $\vec{P}$:

$$\vec{P} = \left\{ b_{31}\left[\frac{b_{23}b_{12} - b_{13}\left(b_{22}+\omega^2\right)}{\left(b_{11}+\omega^2\right)\left(b_{22}+\omega^2\right) - b_{12}b_{21}}\right] + b_{32}\left[\frac{b_{13}b_{21} - b_{23}\left(b_{11}+\omega^2\right)}{\left(b_{11}+\omega^2\right)\left(b_{22}+\omega^2\right) - b_{12}b_{21}}\right] + b_{33}\right\}\vec{E}. \tag{9}$$

The dielectric function of the TMC then can be written as

$$\varepsilon(\omega) = 1 + \chi(\omega)/\varepsilon_0, \tag{10}$$

where

$$\chi(\omega) = \left\{ b_{31}\left[\frac{b_{23}b_{12} - b_{13}\left(b_{22}+\omega^2\right)}{\left(b_{11}+\omega^2\right)\left(b_{22}+\omega^2\right) - b_{12}b_{21}}\right] + b_{32}\left[\frac{b_{13}b_{21} - b_{23}\left(b_{11}+\omega^2\right)}{\left(b_{11}+\omega^2\right)\left(b_{22}+\omega^2\right) - b_{12}b_{21}}\right] + b_{33}\right\}. \tag{11}$$

And the implied dispersion relation of bulk phonon–polaritons is then given by

$$\frac{k^2c^2}{\omega^2} = 1 + \chi(\omega)/\varepsilon_0. \tag{12}$$

Solving equation (12) with (11), one can obtain generally three frequencies of phonon–polaritons propagated in such a TMC system as functions of the wavevector k. Naturally the frequencies also depend on the composition x.

We have calculated numerically the frequencies of bulk phonon–polaritons for several TMCs of III–V, II–VI compound semiconductors with various compositions x. As examples, the phonon–polariton dispersion curves for the TMC systems $Al_xGa_{1-x}As$, $Zn_xCd_{1-x}S$, and $Ga_xIn_{1-x}N$ are illustrated in figure 1, where the composition x is chosen successively as 0, 0.38, 1; 0, 0.5, 1; and 0, 0.5, 1 for the three systems. The used parameters are listed in table 1.

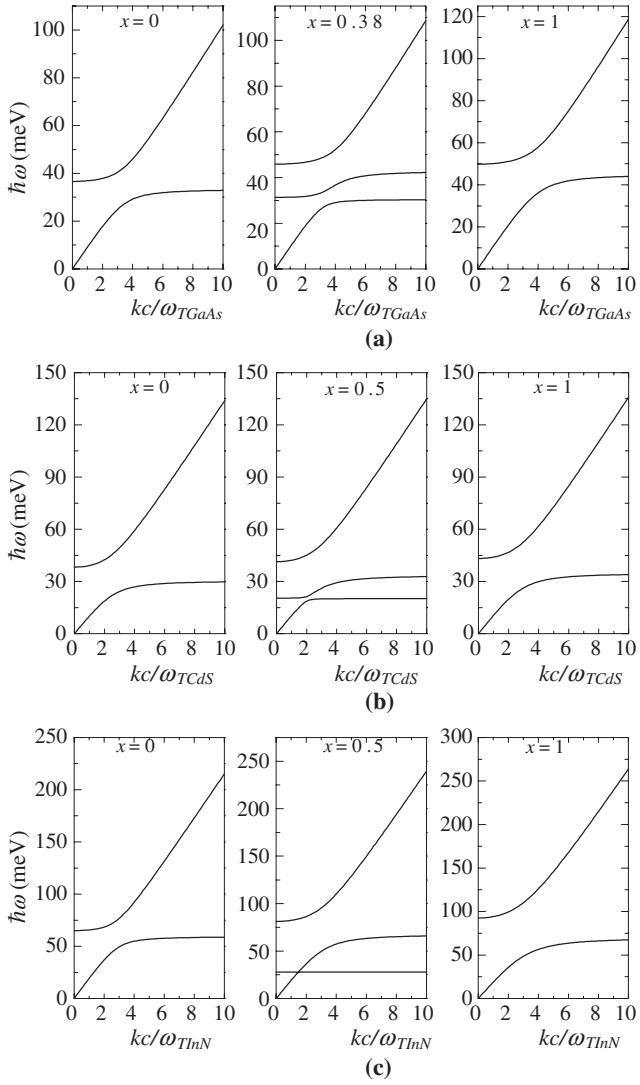

Figure 1. Energies of the bulk phonon–polaritons as functions of the wavevectors for (a) $Al_xGa_{1-x}As$, (b) $Zn_xCd_{1-x}S$, and (c) $Ga_xIn_{1-x}N$. The dimensionless wavevector $kc/\omega_{\mathrm{TGaAs}}$, $kc/\omega_{\mathrm{TCdS}}$, and $kc/\omega_{\mathrm{TInN}}$ are used, where ω_{TGaAs}, ω_{TCdS}, and ω_{TInN} are the frequencies of TO phonons for systems (a), (b), and (c), and c the velocity of light.

As was expected, the dispersion curves of TMCs degenerate respectively to those of the corresponding binary crystals GaAs, CdS, and InN when $x = 0$ and AlAs, ZnS, and GaN when $x = 1$, where there are only two branches of polariton dispersion curves. When the composition x is neither zero nor one, dispersion characteristics different qualitatively from those in binary crystals can be found. It is clearly seen that there are three branches of phonon–polariton frequencies in the figures.

As $k \to 0$, one of the three solutions (photo-like branch) has vanishing frequency similar to that in binary systems, but the others get finite frequencies. The two finite frequencies correspond to respectively the lower ($\omega_{1\mathrm{L}}$) and upper ($\omega_{2\mathrm{L}}$) branches of long-wavelength LO

Table 1. Optical phonon energies, dielectric constants, effective masses of electrons, and the lattice constants for binary materials. Energy is measured in meV, m in the electron rest mass, and the lattice constants in nm.

Materials	$\hbar\omega_{TO}$	$\hbar\omega_{LO}$	ε_0	ε_∞	m	M (au)		a
AlAs[a]	44.88	50.09	10.06	8.16	0.150	26.99	74.92	0.5660[c]
GaAs[a]	33.29	36.25	13.18	10.89	0.067	69.72	74.92	0.56419[c]
ZnS[b]	34.65	44.00	8.00	5.14	0.280	65.38	32.06	0.5410[c]
CdS[b]	30.25	38.24	8.42	5.27	0.155	112.4	32.06	0.5825[c]
GaN[d]	69.43	91.87	9.5	5.35	0.20	69.72	14.01	0.5185[c]
InN[d]	59.27	86.05	9.3	7.72	0.11	114.8	14.01	0.5760[c]

[a] Reference [31].
[b] Reference [32].
[c] Reference [33].
[d] Reference [22].

Table 2. Calculated bulk and surface optical phonon energies for several ternary mixed crystals. Energy is measured in meV.

Material	$h\omega_{1S}$	$h\omega_{2S}$	$h\omega_{1L}$	$h\omega_{1T}$	$h\omega_{2L}$	$h\omega_{2T}$
$Al_{0.38}Ga_{0.62}As$	31.22	45.54	31.28	30.37	45.84	42.72
$Zn_{0.5}Cd_{0.5}S$	20.37	40.19	20.39	20.18	41.38	33.36
$Ga_{0.5}In_{0.5}N$	27.85	79.48	27.87	27.84	81.22	67.30

phonons of the TMCs, for which $\varepsilon(\omega) = 0$. As $k \to \infty$, the frequencies of two lower branches of polaritons finally tend to respectively the frequencies of the lower (ω_{1T}) and upper (ω_{2T}) branches of long-wavelength TO phonons of the TMCs, and the highest one (photo-like branch) to infinity. The mode frequencies of TO and LO phonon branches in the TMCs were calculated with various methods [25, 29, 30] and here we list our results for the above-mentioned systems in table 2.

Moreover, the phonon–polariton dispersion curves in figure 1 show so-called 'two-mode' and 'one-mode' behaviours respectively for different systems. The TMC $Al_{0.38}Ga_{0.62}As$ shows its 'two-mode' behaviour in the dispersion curves. For this kind of system, we have two TO–LO pairs of frequency branches of optical phonons, i.e. ω_{1T}–ω_{1L} and ω_{2T}–ω_{2L} pairs, and in succession $\omega_{2L} > \omega_{2T} > \omega_{1L} > \omega_{1T}$, so that the propagated polariton modes are divided into three frequency regions (propagated bands) by two forbidden bands from ω_{1T} to ω_{1L} and ω_{2T} to ω_{2L} respectively, where no phonon–polariton modes exist.

Otherwise, the 'one-mode' behaviour of optical vibrations is shown by the phonon–polariton dispersion curves of the TMC systems $Zn_{0.5}Cd_{0.5}S$ and $Ga_{0.5}In_{0.5}N$. For this kind of system we have only one TO(ω_{2T})–LO(ω_{2L}) pair of optical-phonon branches, whose frequencies are obviously separate. The frequencies in the other TO(ω_{1T})–LO(ω_{1L}) pair are close to each other, so that the corresponding forbidden band is nearly a horizontal line, whose frequency falls in the lower propagated band. Therefore only one forbidden band for the phonon–polariton propagation can be observed in these systems.

For ease of representation, we have also numerically calculated the oscillator strengths of the polaritons as functions of the composition x in the TMCs $Al_xGa_{1-x}As$, $Zn_xCd_{1-x}S$, and $Ga_xIn_{1-x}N$, and the numerical results are plotted in figure 2. It is seen that the oscillator strengths of two branches of polaritons, the AlAs-like (the upper) and GaAs-like (the lower) modes, have the same order of magnitude and increase non-linearly with increasing the mole fraction of the Al and Ga components respectively in the $Al_xGa_{1-x}As$ system. Therefore, the

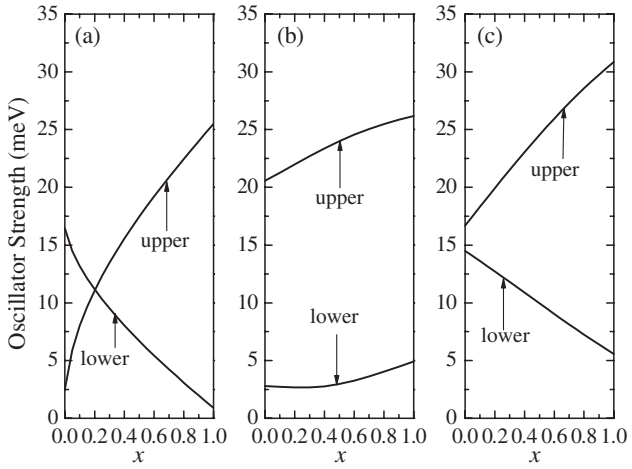

Figure 2. Oscillator strengths of the bulk phonon–polaritons as functions of the composition x for (a) $Al_xGa_{1-x}As$, (b) $Zn_xCd_{1-x}S$, and (c) $Ga_xIn_{1-x}N$.

two branches of oscillators are both observable and the system shows the 'two-mode' behaviour of optical vibrations.

On the other hand, for the TMC systems $Zn_xCd_{1-x}S$ and $Ga_xIn_{1-x}N$ in figures 2(b) and (c), the oscillator strength of the upper branch of polaritons is obviously greater than the lower one. The latter has oscillator strength too weak to be observed. Therefore only the upper branch of oscillators is observable, so the systems are of 'one-mode' behaviour.

3. Surface phonon–polaritons in ternary mixed crystals

In the above discussion, we have mentioned a bulk system, where polaritons propagate in an infinite TMC material and all the effects associated with the surfaces are ignored. Now we turn to discuss the surface modes of phonon–polaritons. Consider a semi-infinite TMC occupying the half-space of $z < 0$ and a phonon–polariton propagates along the surface between the vacuum and the TMC with the two-dimensional wavevector $\vec{k}_\parallel$. For convenience we choose the wavevector $\vec{k}_\parallel$ along the x direction, i.e. $k_x = k_\parallel$ and $k_y = 0$, without loss of generality. In the present geometry, only the surface polaritons of transverse magnetic (TM) character need to be considered. The electric field $\vec{E}$ lies in the x–z plane and the magnetic field $\vec{H}$ is along the y-axis. Mills and Maradudin have investigated the polaritons in a film of binary crystal material and obtain surface modes of phonon–polaritons [3]. Here we extend their theory to the case of semi-infinite TMC systems. For ease of statement, we rewrite here main results given by Mills and Maradudin. To describe the solutions localized in the vicinity of the surface of the material, the field $\vec{E}$ is chosen as the following form:

$$E = \begin{cases} E^{(1)} \exp\left(\mathrm{i}k_\parallel x - \kappa_1 z\right) \mathrm{e}^{-\mathrm{i}\omega t} & z > 0 \\ E^{(2)} \exp\left(\mathrm{i}k_\parallel x + \kappa_2 z\right) \mathrm{e}^{-\mathrm{i}\omega t} & z < 0 \end{cases} \tag{13}$$

which decays exponentially to zero as $z \to \pm\infty$, where κ_1 and κ_2 are respectively the decay constants of the surface waves in the vacuum and TMC material and both real and positive to keep the waves decaying with departing from the surface. They are determined by the following equation:

$$\kappa_i^2 = k_\parallel^2 - \varepsilon_i\ (\omega)\, \omega^2/c^2 \qquad (i = 1, 2). \tag{14}$$

Using the continuity boundary condition, the relation between the dielectric functions of media '1' and '2' is obtained as

$$\varepsilon_2(\omega)/\kappa_2 = -\varepsilon_1/\kappa_1. \tag{15}$$

Denoting that medium '1' is a vacuum and $\varepsilon_1 = 1$, we finally have the equation

$$\varepsilon(\omega)/\kappa_2 = -1/\kappa_1. \tag{16}$$

Substituting equation (14) into (16) one can obtain the implied dispersion equation for the surface phonon–polaritons

$$k_\parallel^2 c^2/\omega^2 = \varepsilon\,(\omega)/[1 + \varepsilon\,(\omega)], \tag{17}$$

where $\varepsilon(\omega)$ is the dielectric function of the TMC depending on the polariton frequency ω. It is evident from equation (16) that the surface polariton waves can exist only in the region of frequencies where $\varepsilon(\omega) < 0$.

By using the corresponding expressions of equations (10) and (11) in section 2 for the dielectric function $\varepsilon(\omega)$ in the TMC, equation (16) can be solved numerically and gives the frequencies of the surface phonon–polaritons as functions of the wavevector $k_\parallel$ as well as the composition x. The computed results for the systems $Al_xGa_{1-x}As$, $Zn_xCd_{1-x}S$, and $Ga_xIn_{1-x}N$ are illustrated in figure 3.

The dispersion curves of surface phonon–polaritons in figure 3 show characteristics quite different from those in bulk materials and binary systems. When $x = 0$ and 1, the dispersion curves degenerate to those of the binary end-materials: there is only one branch of surface phonon–polariton frequency lying between ω_{TO} and ω_{LO} in the forbidden band for the bulk phonon–polariton. When the composition x is neither unity nor zero, the dispersion curves display their TMC characteristics: two branches of surface phonon–polariton frequencies as well as the 'two-mode' and 'one-mode' behaviours.

It is found in figure 3(a) that there are two branches of surface phonon–polariton frequencies lying respectively in the two forbidden bands of bulk phonon–polaritons for the 'two-mode' behaviour TMC $Al_{0.38}Ga_{0.62}As$. The curves start from the frequencies of the upper and lower branches of TO phonons in the bulk TMC at the wavevectors $k_\parallel \to \omega_{2T}/c$ and ω_{1T}/c, and finally tend to two SO-phonon frequencies ω_{2S} (AlAs-like) and ω_{1S} (GaAs-like) as $k_\parallel \to \infty$, respectively. One can find two forbidden bands: from ω_{2S} to ω_{2L} and ω_{1S} to ω_{1L}, where neither the bulk phonon–polariton modes nor the surface modes can be propagated. The width of the forbidden band of GaAs-like modes (the lower one) is around 0.9 meV, which is one-third of that of AlAs-like modes (about 3.2 meV). This results in that the Raman scattering peak by the surface phonon–polariton mode of the lower branch may be hidden in the tail of the bulk modes. Therefore we guess that the upper branch of the surface phonon–polaritons for the semi-infinite $Al_{0.38}Ga_{0.62}As$ is expected to be easily observed, but the lower one slightly difficult.

Figures 3(b) and (c) show the one-mode behaviour characteristics of the surface phonon–polaritons in the TMCs $Zn_{0.5}Cd_{0.5}S$ and $Ga_{0.5}In_{0.5}N$. There is only one observable branch of surface phonon–polaritons between ω_{2T} and ω_{2L}, corresponding to the forbidden band of the upper branch of bulk modes. The widths of the upper forbidden bands are 8 and 12 meV for $Zn_{0.5}Cd_{0.5}S$ and $Ga_{0.5}In_{0.5}N$ respectively, so that the corresponding surface modes could be observed. However, the curve of the lower branch of surface polaritons is nearly a horizontal line, whose frequency falls in the lower bulk-polariton propagated bands, so that cannot be observed independently.

To understand clearly the 'two-mode' and 'one-mode' mode behaviours of surface modes in TMCs, we have also calculated the frequencies of SO phonons for several TMC systems. Let

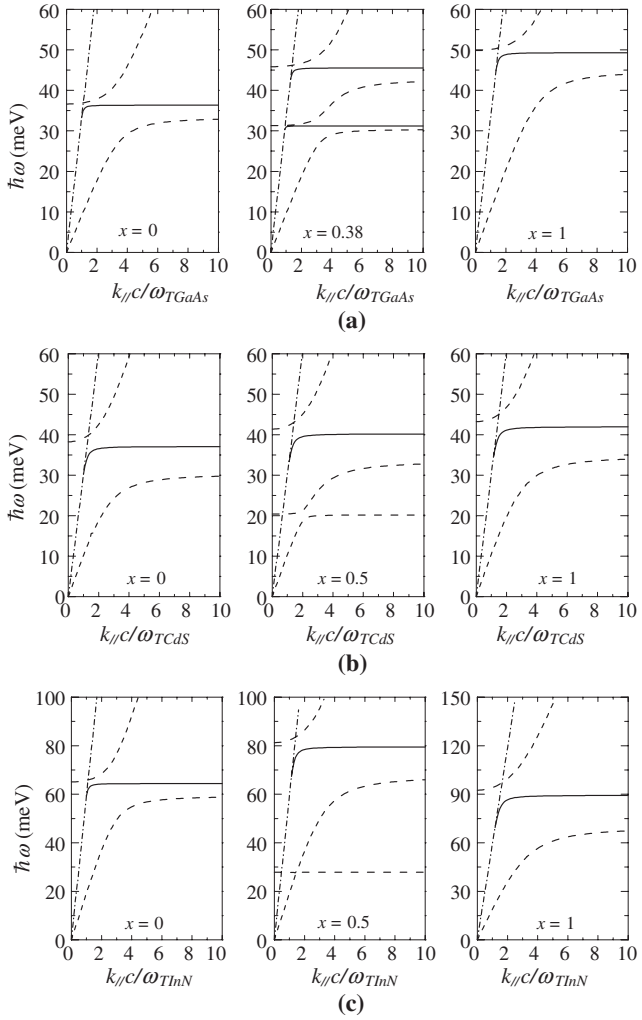

Figure 3. Energies of the surface phonon–polaritons (solid lines), bulk phonon–polaritons (long-dashed), and the 'photons' (dashed–dotted) as functions of the wavevector $k_\parallel$ for (a) $Al_xGa_{1-x}As$, (b) $Zn_xCd_{1-x}S$, and (c) $Ga_xIn_{1-x}N$. Dimensionless wavevectors the same as those in figure 1 are used.

$\kappa_1 = \kappa_2 = k_\parallel$ in equation (16); one can obtain the following equation satisfied by SO phonon modes in a 'semi-infinite' TMC:

$$\varepsilon(\omega) = -1. \tag{18}$$

Solving numerically equation (18) with (10) and (11), we obtain the SO phonon frequencies as functions of the composition x for $Al_xGa_{1-x}As$, $Zn_xCd_{1-x}S$, and $Ga_xIn_{1-x}N$ systems and the results are illustrated in figure 4.

For the 'two-mode' behaviour TMC $Al_xGa_{1-x}As$ in figure 4(a), two branches of observable SO-phonon frequencies, ω_{1S} and ω_{2S}, lie between the LO and TO modes respectively subject to the GaAs-like (the lower) and AlAs-like (the upper) LO–TO pairs. On the other hand, the surface modes also show their 'one-mode' behaviour in $Zn_xCd_{1-x}S$ and $Ga_xIn_{1-x}N$ systems (see figures 4(b) and (c)). The branch of SO-phonon modes with the higher

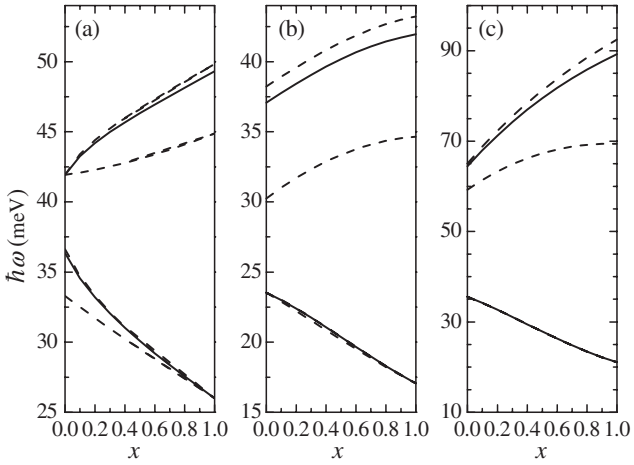

Figure 4. Calculated frequencies of surface optical phonons (solid lines) for (a) $Al_xGa_{1-x}As$, (b) $Zn_xCd_{1-x}S$, and (c) $Ga_xIn_{1-x}N$. The dashed lines are the frequencies of bulk optical phonons.

frequencies ω_{2S} is dominant in this kind of system. Its frequency changes continuously from ω_{SB} of CdS (or InN) at $x = 0$ to ω_{SA} of crystal ZnS (or GaN) at the other end. Another branch with the lower frequencies ω_{1S} is not important because of the very weak oscillator strength.

4. Conclusion

We have investigated theoretically the bulk and surface phonon–polaritons of TMCs in the MREI model and the Born–Huang approximation. The frequencies and oscillator strengths of the bulk and surface phonon–polaritons have been calculated. It is found from the numerical results for TMCs $Al_xGa_{1-x}As$, $Zn_xCd_{1-x}S$, and $Ga_xIn_{1-x}N$ that there are three frequency branches and two forbidden bands for the bulk phonon–polaritons in TMC systems. Two branches of surface phonon–polaritons are also found in semi-infinite TMC systems. The 'two-mode' and 'one-mode' behaviours of phonon–polaritons are also shown in the dispersion curves of bulk and surface phonon–polaritons.

It should be pointed out that we have considered the III-nitride (III-N) system $Ga_xIn_{1-x}N$ in NaCl structure to discuss their bulk and surface phonon–polaritons. In fact, the III-N compounds are usually grown in a wurtzite structure, which is not of a cubic lattice. The more accurate calculation for III-N TMCs should take the anisotropy into account and will be a subject of future investigations.

Acknowledgments

This work was supported in part by the PhD Progress Foundation of higher education institutions of China (No 20040126003) and the Natural Science Foundation of Inner Mongol of China (No 200408020101).

Appendix

The expressions for the dynamical coefficients b_{ij} $(i, j = 1, 2, 3)$ in equations (5)–(7) can be determined by the following formulae [29, 30]:

$$b_{11} = -\omega_{\mathrm{TA}}^2\eta_{\mathrm{A}}\frac{M_{\mathrm{C}}+M_{\mathrm{A}}x}{M_{\mathrm{C}}+M_{\mathrm{A}}} + \omega_{\mathrm{TA}}\Bigg[\omega_{\mathrm{TA}}\kappa_{\mathrm{A}}\sigma_{\mathrm{A}}\frac{M_{\mathrm{C}}+M_{\mathrm{A}}x}{M_{\mathrm{C}}+M_{\mathrm{A}}} + \omega_{\mathrm{TB}}\left(\kappa_{\mathrm{A}}\kappa_{\mathrm{B}}\sigma_{\mathrm{A}}\sigma_{\mathrm{B}}\mu_{\mathrm{B}}/\mu_{\mathrm{A}}\right)^{1/2}\frac{M_{\mathrm{A}}(1-x)}{M_{\mathrm{C}}+M_{\mathrm{A}}}\Bigg]xa(x), \tag{A.1}$$

$$b_{12} = -\omega_{\mathrm{TB}}^2\eta_{\mathrm{B}}\frac{M_{\mathrm{B}}(1-x)}{M_{\mathrm{C}}+M_{\mathrm{B}}}\left(\mu_{\mathrm{A}}/\mu_{\mathrm{B}}\right)^{1/2} + \omega_{\mathrm{TB}}\Bigg[\omega_{\mathrm{TB}}\kappa_{\mathrm{B}}\sigma_{\mathrm{B}}\left(\mu_{\mathrm{B}}/\mu_{\mathrm{A}}\right)^{1/2}\frac{M_{\mathrm{A}}(1-x)}{M_{\mathrm{C}}+M_{\mathrm{A}}} + \omega_{\mathrm{TA}}\left(\kappa_{\mathrm{A}}\kappa_{\mathrm{B}}\sigma_{\mathrm{A}}\sigma_{\mathrm{B}}\right)^{1/2}\frac{M_{\mathrm{C}}+M_{\mathrm{A}}x}{M_{\mathrm{C}}+M_{\mathrm{A}}}\Bigg](1-x)a(x), \tag{A.2}$$

$$b_{13} = \left[\omega_{\mathrm{TA}}\left(\kappa_{\mathrm{A}}\sigma_{\mathrm{A}}\right)^{1/2}\frac{M_{\mathrm{C}}+M_{\mathrm{A}}x}{M_{\mathrm{C}}+M_{\mathrm{A}}} + \omega_{\mathrm{TB}}\left(\kappa_{\mathrm{B}}\sigma_{\mathrm{B}}\mu_{\mathrm{B}}/\mu_{\mathrm{A}}\right)^{1/2}\frac{M_{\mathrm{A}}(1-x)}{M_{\mathrm{C}}+M_{\mathrm{A}}}\right]\varepsilon_0^{1/2}a(x), \tag{A.3}$$

$$b_{21} = -\omega_{\mathrm{TA}}^2\eta_{\mathrm{A}}\frac{M_{\mathrm{A}}x}{M_{\mathrm{C}}+M_{\mathrm{A}}}\left(\mu_{\mathrm{B}}/\mu_{\mathrm{A}}\right)^{1/2} + \omega_{\mathrm{TA}}\Bigg[\omega_{\mathrm{TA}}\kappa_{\mathrm{A}}\sigma_{\mathrm{A}}\left(\mu_{\mathrm{A}}/\mu_{\mathrm{B}}\right)^{1/2}\frac{M_{\mathrm{B}}x}{M_{\mathrm{C}}+M_{\mathrm{B}}} + \omega_{\mathrm{TB}}\left(\kappa_{\mathrm{A}}\kappa_{\mathrm{B}}\sigma_{\mathrm{A}}\sigma_{\mathrm{B}}\right)^{1/2}\frac{M_{\mathrm{C}}+M_{\mathrm{B}}(1-x)}{M_{\mathrm{C}}+M_{\mathrm{B}}}\Bigg]xa(x), \tag{A.4}$$

$$b_{22} = -\omega_{\mathrm{TB}}^2\eta_{\mathrm{B}}\frac{M_{\mathrm{C}}+M_{\mathrm{B}}(1-x)}{M_{\mathrm{C}}+M_{\mathrm{B}}} + \omega_{\mathrm{TB}}\Bigg[\omega_{\mathrm{TB}}\kappa_{\mathrm{B}}\sigma_{\mathrm{B}}\frac{M_{\mathrm{C}}+M_{\mathrm{B}}(1-x)}{M_{\mathrm{C}}+M_{\mathrm{B}}} + \omega_{\mathrm{TA}}\left(\kappa_{\mathrm{A}}\kappa_{\mathrm{B}}\sigma_{\mathrm{A}}\sigma_{\mathrm{B}}\mu_{\mathrm{A}}/\mu_{\mathrm{B}}\right)^{1/2}\frac{M_{\mathrm{B}}x}{M_{\mathrm{C}}+M_{\mathrm{B}}}\Bigg](1-x)a(x), \tag{A.5}$$

$$b_{23} = \left[\omega_{\mathrm{TB}}\left(\kappa_{\mathrm{B}}\sigma_{\mathrm{B}}\right)^{1/2}\frac{M_{\mathrm{C}}+M_{\mathrm{B}}(1-x)}{M_{\mathrm{C}}+M_{\mathrm{B}}} + \omega_{\mathrm{TA}}\left(\kappa_{\mathrm{A}}\sigma_{\mathrm{A}}\mu_{\mathrm{A}}/\mu_{\mathrm{B}}\right)^{1/2}\frac{M_{\mathrm{B}}x}{M_{\mathrm{C}}+M_{\mathrm{B}}}\right]\varepsilon_0^{1/2}a(x), \tag{A.6}$$

$$b_{31} = \omega_{\mathrm{TA}}\left(\kappa_{\mathrm{A}}\sigma_{\mathrm{A}}\right)^{1/2}\varepsilon_0^{1/2}xa(x), \tag{A.7}$$

$$b_{32} = \omega_{\mathrm{TB}}\left(\kappa_{\mathrm{B}}\sigma_{\mathrm{B}}\right)^{1/2}\varepsilon_0^{1/2}(1-x)a(x), \tag{A.8}$$

$$b_{33} = \varepsilon_0[a(x)-3], \tag{A.9}$$

where

$$a(x) = 3/[1-\gamma_{\mathrm{A}}\sigma_{\mathrm{A}}x - \gamma_{\mathrm{B}}\sigma_{\mathrm{B}}(1-x)]$$

$$\sigma_l \equiv v_l/v, \qquad \gamma_l = \frac{\varepsilon_{\infty l}-1}{\varepsilon_{\infty l}+2}, \qquad \kappa_l = \frac{\varepsilon_{sl}-\varepsilon_{\infty l}}{(\varepsilon_{\infty l}+2)^2},$$
$$\eta_l = \frac{\varepsilon_{sl}+2}{\varepsilon_{\infty l}+2}, \qquad (l = \mathrm{A}, \mathrm{B}).$$

In the above equations, ε_{sl} and $\varepsilon_{\infty l}$ are respectively the static and optical dielectric constants of the end-member materials (AC for $l = \mathrm{A}$ and BC for $l = \mathrm{B}$). ω_{TA} and ω_{TB} are respectively the TO-phonon frequencies of AC and BC. M_{A}, M_{B}, and M_{C} are respectively the masses of ions A, B, and C. The reduced masses are given by

$$\mu_{\mathrm{A}} = \frac{M_{\mathrm{C}}M_{\mathrm{A}}}{M_{\mathrm{C}}+M_{\mathrm{A}}}, \qquad \text{and} \qquad \mu_{\mathrm{B}} = \frac{M_{\mathrm{C}}M_{\mathrm{B}}}{M_{\mathrm{C}}+M_{\mathrm{B}}}.$$

Here M_{A}, M_{B}, and M_{C} are respectively the masses of ions A, B, and C, v is the volume of the unit-cell of the TMC, and v_{A} and v_{B} are respectively the unit-cell volume of the end-member crystals AC and BC.

References

[1] Born M and Huang K 1954 *Dynamical Theory of Crystal Lattices* (New York: Oxford University Press)
[2] Henry C H and Hopfield J J 1965 *Phys. Rev. Lett.* **15** 964

[3] Mills D L and Maradudin A A 1973 *Phys. Rev. Lett.* **31** 372
[4] Mills D L and Burstein E 1974 *Rep. Prog. Phys.* **37** 817
[5] Watanabe J, Uchinokura K and Sekine T 1989 *Phys. Rev.* B **40** 5677
[6] Comas F, Gine C T and Cardona M 1997 *Phys. Rev.* B **56** 4115
[7] Huang K C, Bienstman P, Joannopoulos J D, Nelson K A and Fan S 2003 *Phys. Rev.* B **68** 075209
[8] Zhang X J, Zhu R Q, Zhao J, Chen Y F and Zhu Y Y 2004 *Phys. Rev.* B **69** 085118
[9] Marschall N and Fischer B 1972 *Phys. Rev. Lett.* **28** 811
[10] Barker A S 1972 *Phys. Rev. Lett.* **28** 892
[11] Watanabe J, Uchinokura K and Sekine T 1989 *Phys. Rev.* B **40** 7860
[12] Shen Y R and Bloembergen N 1965 *Phys. Rev.* **137** A1787
[13] Gale G M, Vallee F and Flytzanis C 1986 *Phys. Rev. Lett.* **57** 1867
[14] Stepanov A G, Hebling J and Kuhl J 2001 *Phys. Rev.* B **63** 104304
[15] Hebling J 2002 *Phys. Rev.* B **65** 092301
[16] Wahlstrand J K and Merlin R 2003 *Phys. Rev.* B **68** 054301
[17] Kojima S, Tsumura N, Takeda M W and Nishizawa S 2003 *Phys. Rev.* B **67** 035102
[18] Farjima S S, Soltani B and Hadari K 2002 *Int. J. Infrared Millim. Waves* **23** 1455
[19] Farjima S S and Solimany M A 2003 *Int. J. Infrared Millim. Waves* **24** 61
[20] Taylor D W 1988 *Optical Properties of Mixed Crystals* ed R J Elliot and I P Ipatova (Amsterdam: North-Holland) chapter 2
[21] Kim K W and Stroscio M A 1990 *J. Appl. Phys.* **68** 6289
[22] Yu S, Kim K W, Bergman L, Dutta M, Stroscio M A and Zavada J M 1998 *Phys. Rev.* B **58** 15283
[23] Jimènez-Sandoval S, Lòpez-Rivera A and Irwin J C 2003 *Phys. Rev.* B **68** 054303
[24] Szybowicz M, Kozielski M, Firszt F, Legowski S and Meczynska H 2003 *Cryst. Res. Technol.* **38** 359
[25] Chang I F and Mitra S S 1971 *Adv. Phys.* **20** 359
[26] Lu Y Q, Zhu Y Y, Chen Y F, Zhu S N, Ming N B and Feng Y J 1999 *Science* **284** 1822
[27] Zhu Y Y, Zhang X J, Lu Y Q, Chen Y F, Zhu S N and Ming N B 2003 *Phys. Rev. Lett.* **90** 053903
[28] Masale M 2003 *Semicond. Sci. Technol.* **18** 480
Masale M 2003 *Semicond. Sci. Technol.* **19** 1358
[29] Liang X X and Ban S L 2004 *Chin. Phys.* **13** 71
[30] Liang X X and Yang J S 1996 *Solid State Commun.* **100** 629
[31] Adachi S 1985 *J. Appl. Phys.* **58** R1
[32] Kartheuser E 1973 *Polarons in Ionic Crystals and Polar Semiconductors* ed J T Devreese (Amsterdam: North-Holland) p 718
[33] Strite S and Morkoc H 1992 *J. Vac. Sci. Technol.* B **10** 1237